JOC*Article*

Conformational Properties, Chiroptical Spectra, and Molecular Self-Assembly of 2,3-Piperazinodiones and Their Dithiono Analogues

Barbara Piotrkowska,[†] Małgorzata Myślińska,[†] Maria Gdaniec,[‡] Aleksander Herman,[†] and Tadeusz Połoński*,[†]

Department of Chemistry, Technical University, 80-952 Gdańsk, Poland, and Faculty of Chemistry, A. Mickiewicz University, 60-780 Poznań, Poland

tadpol@chem.pg.gda.pl

Received January 7, 2008

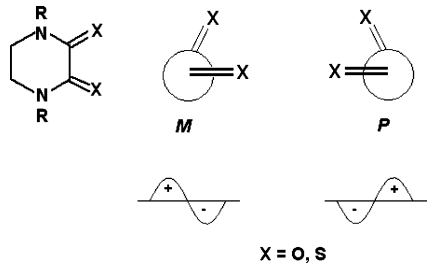

A family of chiral cyclic oxamides was prepared by the condensation of optically active 1,2-diamines with diethyl oxalate. Thionation of the products with Lawesson's reagent afforded a series of chiral 2,3-piperazinedithiones. Molecular geometries of the title compounds were studied with the use of quantum mechanical DFT calculations and were compared to the X-ray crystallographic results. The heterocyclic six-membered ring adopted a half-chair conformation with the C-5 substituent preferably at the equatorial position, whereas a substitution at the nitrogen atoms resulted in domination of the axial form in the conformational equilibrium. The opposite helicity of the twisted oxamide chromophore in the axial and equatorial conformers led to the opposite signs of the Cotton effects corresponding to two $\pi-\pi^*$ electronic transitions. The CD signs can be predicted by a simple helicity rule. The same rule is valid for 2,3-piperazinodithiones, where a substitution of sulfur for oxygen in the carbonyl groups results in bathochromic shifts of the absorption and CD bands. The crystal packing analysis of several 2,3-piperazinodiones revealed that strong NH···O═C intermolecular hydrogen-bonding interactions generating the chain motif resulted in the formation of 3-D networks as well as with the use of the cyclic hydrogen-bond motif tape structures.

Introduction

Oxamides and dithioxamides represent an important class of compounds with relevance in many areas of chemistry. Simple oxamides, due to their ability of self-complementary hydrogen-bonding interactions, have been used successfully in materials science as supramolecular building blocks for the construction of ordered solid state assemblies,[1] helicate structures,[2] and gelators yielding thermo-reversible gels.[3] The oxamide unit has gained considerable importance in the design of modified peptide and protein structures. It has been shown that the selective substitution of one or more amide groups by oxamide units changes the folding properties of the peptide backbone and thus can be envisaged as a potential strategy in protein engineering.[4] The most familiar application of dithiooxamides is their use as reagents for the detection and determination of

* Corresponding author. Fax: (48)-58-3472694.
[†] Technical University.
[‡] A. Mickiewicz University.

(1) (a) Coe, S.; Kane, J. J.; Nguyen, T. L.; Toledo, L. M.; Wininger, E.; Fowler, F. W.; Lauher, J. W. *J. Am. Chem. Soc.* **1997**, *119*, 86. (b) Nguyen, T. L.; Scott, A.; Dinkelmeyer, B.; Fowler, F. W.; Lauher, J. W. *New. J. Chem.* **1998**, 129. (c) Nguyen, T. L.; Fowler, F. W.; Lauher, J. W. *J. Am. Chem. Soc.* **2001**, *123*, 11057.

(2) (a) Blay, G.; Fernandez, I.; Pedro, J. R.; Ruiz-Garcia, R.; Carmen-Munoz, M.; Cano, J.; Carrasco, R. *Eur. J. Org. Chem.* **2003**, 1627. (b) Piotrkowska, B.; Milewska, M. J.; Gdaniec, M.; Połoński, T. *Tetrahedron: Asymmetry* **2007**, *18*, 1486.

(3) (a) Makarević, J.; Jokić, M.; Perić, B.; Tomisić, V.; Kojić-Prodić, B.; Zinić, M. *Chem.—Eur. J.* **2001**, *7*, 3328. (b) Makarević, J.; Jokić, M.; Frkanec, L.; Katalenić, D.; Zinić, M. *Chem. Commun. (Cambridge, U.K.)* **2002**, 2238. (c) Makarević, J.; Jokić, M.; Raza, Z.; Stefanić, Z.; Kojić-Prodić, B.; Zinić, M. *Chem.—Eur. J.* **2003**, *9*, 5567.

10.1021/jo800037w CCC: $40.75
Published on Web 03/12/2008

various metals.[5] On the other hand, *N*,*N*′-disubstituted oxamides have played a key role in the design of polymetallic and heterobimetallic complexes.[6]

Oxamides and dithiooxamides have been a subject of interest to photochemists and spectroscopists for the last four decades, and they have been investigated by various spectroscopic methods.[7] These chromophores are composed of two amide or thioamide subunits, and their interaction lifts degeneracy between pairs of the *n*, π, and π^* levels. The interaction between the carbonyl or the thiocarbonyl groups and thus splitting of these levels is strongly influenced by the geometry of the oxamide or dithiooxamide chromophore. According to X-ray crystallographic studies, unsubstituted and *N*,*N*′-disubstituted oxamides and dithiooxamides assume a planar s-trans conformation,[8a−d] whereas tetrasubstituted compounds, due to steric interactions, prefer twisted conformations.[8e,f] However, the oxamide unit incorporated in some cyclic systems is forced to adopt an s-cis or twisted s-cis conformation.[9] The twisted oxamide and dithioxamide chromophores are inherently chiral, and in the case of *N*,*N*,*N*′,*N*′-tetramethyldithiooxamide, the energy barrier to racemization is sufficiently high to separate to enantiomers at ambient temperature.[10] It has been shown that the six- and seven-membered cyclic oxamides and their dithio analogues also contain the twisted chromophores.[8e,f] We focused our interest on the conformational and chiroptical properties of 2,3-piperazinodiones and their dithio analogues. Attractive characteristics of these compounds are their ease of preparation, crystallinity, and restricted conformational flexibility. Furthermore, a long wavelength absorption of 2,3-piperazinodithiones resulting from the substitution of sulfur for oxygen in the carbonyl groups makes these compound particularly useful as models for spectroscopic studies.[11]

In this paper, we describe the synthesis, structure, and CD spectra of several model compounds, including those with rigid bicyclic skeletons (**1** and **2**) and more flexible ones (**3**−**6**). Our aim was to examine their CD spectra to correlate the observed Cotton effect (CE) signs with the molecular geometries. The conformational preferences of the molecules were studied with

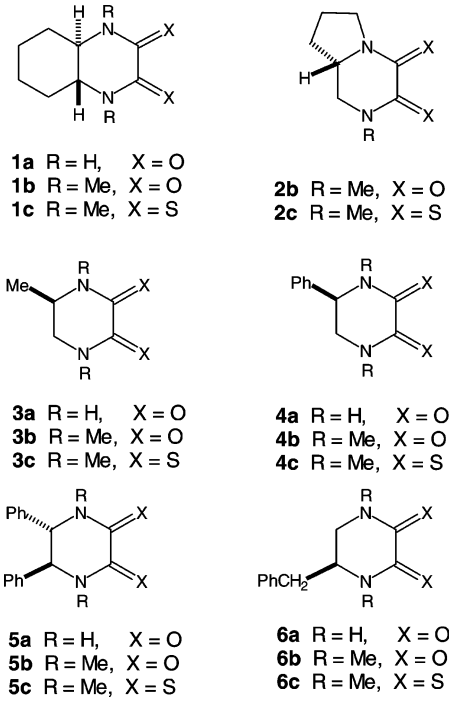

DFT[12] calculations, and the results were compared with those obtained from X-ray crystallographic analysis. In addition, we examined the crystal packing of several 2,3-piperazinediones to establish their self-assembly mode in the solid state.

Results and Discussion

1,3-Piperazinediones **1a**−**6a** were obtained in high yields by the condensation of optically active 1,2-diamines with diethyl oxalate in ethanol following a literature method.[13] Methylation of the products **4a**−**6a** with methyl iodide gave the *N*,*N*′-dimethyl derivatives **4b**−**6b**. Since this procedure failed in the case of **1a** and **3a** with a poor solubility, their *N*,*N*′-dimethyl derivatives **1b** and **3b** were prepared from the corresponding *N*,*N*′-dimethylamines by condensation with diethyl oxalate. Thionation of these compounds with Lawesson's reagent[14] in boiling toluene afforded 1,3-piperazinedithiones **1c**−**6c** (Scheme 1) as dark red crystals.

Molecular Geometry. The 2,3-piperazinedione system may exist in two enantiomeric half-chair conformations with C_2 symmetry and identical energies. Our primary interest was to learn about the influence of substituents on the ring and chromophore geometry that determines the CE sign in the chiroptical spectra. We investigated the structures with the aid of quantum mechanical calculations and X-ray crystallography.

(4) (a) Karle, I. L.; Ranganathan, D. *Biopolymers* **1995**, *46*, 18. (b) Padilla-Martinez, I. I.; Martinez-Martinez, F. J.; Garcia-Baez, E. V.; Rojas-Lima, S.; Höpfl, H. *J. Chem. Soc., Perkin Trans. 2* **2001**, 1817.

(5) (a) Feigel, F. *Spot Tests*; Elsevier: New York, 1954; Vol. 1, pp 83, 139, 145. (b) Welcher, F. J. *Organic Analytical Reagents*; Van Nostrand: New York, 1948; p 148.

(6) (a) Lloret, F.; Sletten, J.; Ruiz, R.; Julve, M.; Faus, J. *Inorg. Chem.* **1992**, *31*, 3778. (b) Sanada, T.; Suzuki, T.; Kaizaki, S. *J. Chem. Soc., Dalton Trans.* **1998**, 959.

(7) (a) Persson, B.; Sandström, J. *Acta Chem. Scand.* **1981**, *35*, 489. (b) Henriksen, L.; Isaksson, R.; Liliefors, T.; Sandström, J. *Acta Chem. Scand.* **1963**, *17*, 1380. (c) Larson, D. B.; McGlynn, S. P. *J. Mol. Spectrosc.* **1973**, *47*, 469. (d) Larson, D. B.; Arnett, J. F.; McGlynn, S. P. *Chem. Phys. Lett.* **1973**, *23*, 322. (e) Isaksson, R.; Liliefors, T. *J. Chem. Soc., Perkin Trans. 2* **1980**, 1815. (f) Green, M. R.; Jubran, N.; Bursten, B. E.; Bush, D. H. *Inorg. Chem.* **1987**, *26*, 2326. (g) Servaas, P. C.; Stufkens, D. J.; Oskam, A.; Vernooijs, P.; Baerends, E. J.; De Ridder, D. J. A.; Stam, C. H. *Inorg. Chem.* **1989**, *28*, 4104.

(8) (a) Romers, C. *Acta Crystallogr.* **1953**, *6*, 429. (b) Ayerst, E. N.; Duke, J. R. C. *Acta Crystallogr.* **1954**, *7*, 588. (c) Wheatley, P. J. *J. Chem. Soc.* **1965**, 396. (d) de With, G.; Harkema, S. *Acta Crystallogr., Sect. B: Struct. Sci.* **1977**, *33*, 2367. (e) Adiwidjaja, G.; Voss, J. *Chem. Ber.* **1977**, *110*, 1159. (f) Lanza, S.; Bruno, G.; Scolaro, L. M.; Nicolo, F.; Rosace, G. *Tetrahedron: Asymmetry* **1993**, *4*, 2311.

(9) Isaksson, R.; Liliefors, T. *J. Chem. Soc., Perkin Trans. 2* **1981**, 1344.

(10) Mannschreck, A.; Talvitie, A.; Fischer, W.; Snatzke, G. *Monatsh. Chem.* **1983**, *114*, 101.

(11) For a preliminary communication, see: Połoński, T. *Tetrahedron: Asymmetry* **1994**, *5*, 149.

(12) (a) Schmidt, M. W.; Baldridge, K. K.; Boatz, J. A.; Elbert, S. T.; Gordon, M. S.; Jensen, J. H.; Koseki, S.; Matsunaga, N.; Nguyen, K. A.; Su, S.; Windus, T. L.; Dupuis, M.; Montgomery, J. A. *J. Comput. Chem.* **1993**, *1347*. (b) Gordon, M. S.; Schmidt, M. W. Advances in Electronic Structure Theory: GAMESS a Decade Later; In *Theory and Applications of Computational Chemistry*; Dykstra, G. E., Frenking, G., Kim, K. S., Scuseria, G. E., Eds.; Elsevier: Amsterdam, 2005 and references therein. (c) Granovsky, A. A. PC GAMESS version 7.1, http://classic.chem.msu.su/gran/gamess/index.html.

(13) Isaksson, R.; Liliefors, T.; Sandström, J. *J. Chem. Res., Synop.* **1981**, 43.

(14) (a) Yde, B.; Yousif, N. M.; Pedersen, V.; Thomsen, J. Lawesson, S.-O. *Tetrahedron* **1984**, *40*, 2047. For a review, see: (b) Cava, M. P.; Levinson, M. J. *Tetrahedron* **1985**, *41*, 5061. (c) Jesberger, M.; Davis, T. P.; Barner, L. *Synthesis* **2003**, 1929. (d) Ozturk, T.; Elas, E.; Mert, O. *Chem. Rev.* **2007**, *107*, 5210.

SCHEME 1

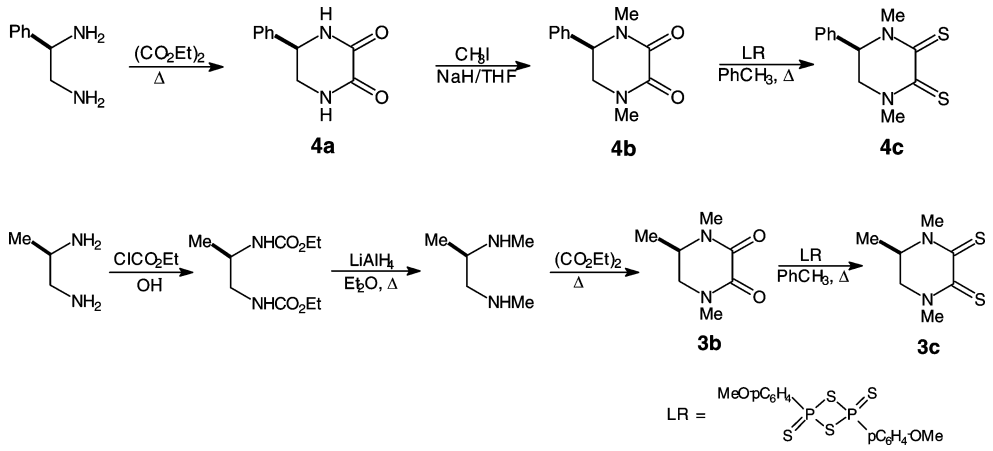

TABLE 1. Selected Torsional Angles and Relative Energies Calculated by DFT[12]

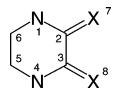

structure[a]	7−2−3−8	1−6−5−4	1−2−3−4	rel energy (kJ/mol)
1a	−20.43	−55.30	−19.87	
1a[b]	−18.7(4)	−56.6(2)	−20.0(4)	
1b	−9.85	−43.51	−10.49	
1c	−37.03	−47.63	−35.69	
3a(eq)	−15.23	−51.83	−14.09	0
3a(ax)	16.47	52.37	15.28	2.5
3a[b]	−20.5(2)	−51.43(16)	−21.0(2)	
3b(eq)	−16.00	−53.81	−16.70	5.9
3b(ax)	18.15	54.44	18.62	0
3b[b]	16.0(2)	52.79(17)	16.1(2)	
3c(eq)	−42.62	−57.43	−39.25	13.1
3c(ax)	35.00	56.78	32.49	0
3c[b]	42.1(2)	56.9(2)	40.2(3)	
4a(eq)	−16.65	−52.15	−15.69	0
4a(ax)	16.69	49.94	16.01	6.8
4*b*(eq)	−13.48	−54.92	−13.90	5.0
4*b*(ax)	15.84	53.16	15.95	0
4c(eq)	−35.67	−56.44	−34.05	7.9
4c(ax)	36.80	55.43	34.27	0
5a(eq)	15.31	49.86	14.02	0
5a(ax)	−17.60	−51.01	−17.49	10.5
5a·THF[b]	−12.4(8)	−57.1(6)	−11.4(7)	
5a·fba·H$_2$O[b]	16.3(4)	52.9(3)	16.2(4)	
5b(eq)	8.30	47.26	8.72	15.8
5b(ax)	−19.36	−54.85	−20.39	0
5b[b]	−9.4(3)	−58.8(2)	−10.0(3)	
	−12.7(4)	−59.3(2)	−13.1(4)	
6a(eq)	14.03	50.90	12.18	1.6
6a(ax)	−15.18	−51.80	−13.99	0
6b(eq)	15.83	53.89	16.46	15.8
6b(ax)	−21.62	−55.77	−22.15	0
6b[b]	−13.9(3)	−52.59(19)	−13.2(3)	
6c(I)[b,c]	−38.52(17)	−57.30(15)	−36.24(19)	
6c(II)[b,d]	−35.4(4)	−56.5(4)	−32.3(5)	
	−30.9(4)	−56.5(4)	−30.8(4)	

[a] DFT calculations [B3LYP RHF GAMESS (version 22) with 6-311G(d,p) basis set]. [b] X-ray analysis. [c] Orthorhombic crystals. [d] Monoclinic crystals.

The calculated and observed geometries of some compounds are compared in Table 1.

A substitution of the heterocyclic ring at C-5 led to two different conformers: one with the substituent at the equatorial position and the other with the axial substituent, and as shown in Scheme 2, they have an opposite helicity of the oxamide unit. Crystal structure analysis revealed that the methyl group in **3a** prefers an equatorial orientation in the solid state (Figure 1a). The six-membered ring is twisted with a N−C5−C6−N torsion angle of −51.43(16)°, and the oxamide chromophore exhibits M-helicity [O═C−C═O is−20.5(2)°]. According to our DFT calculations, the equatorial conformer is 2.5 kJ/mol more stable than the axial conformer and should predominate in solution. However, upon *N*-alkylation, the situation is reversed, and the calculations predicted that the axial conformer of **3b** is preferred over the equatorial conformer by 5.9 kJ/mol. This is apparently due to a destabilizing steric interaction between the equatorial methyl group at C-5 and the nearly coplanar neighboring *N*-methyl substituent. Also, the X-ray structure of **3b** showed that that this compound crystallizes preferably in the axial conformation with the oxamide unit twisted in the P-sense (Figure 1b). An analogous conformational preference was predicted for **4a**,**b** and **5a**,**b** (i.e., a domination of the equatorial form in the case of the NH derivatives and the axial form in the case of the *N*-methyl derivatives), whereas the benzyl group in both derivatives **6a**,**b** prefers an axial orientation. However, in the case of **6a**, the calculated energy difference between two conformers is rather small (1.6 kJ/mol). The X-ray structure of **6b** confirmed an axial orientation of the benzyl substituent. The case of **5a** shows that the energy difference between the axial and the equatorial forms is small and that the packing forces in the crystal can influence the conformation adopted by the 2,3-piperazinedione system in the solid state. This compound was obtained in two crystalline forms, as a solvate with tetrahydrofuran **5a·THF** and as a cocrystal with pentafluorobenzoic acid (**pfb**) **5a·pfb·H$_2$O**. X-ray crystallography revealed that the diaxial form of **5a** is preferred in the solvate, whereas the diequatorial form is observed in the cocrystal with **pfb**. The CD spectra pointed to a predominance of the diequatorial form in solution (vide infra).

SCHEME 2

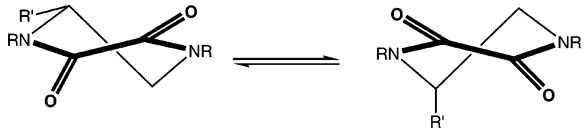

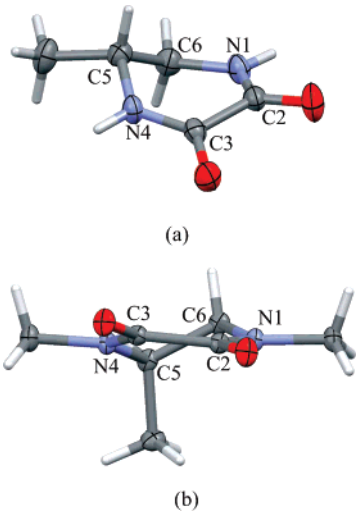

FIGURE 1. Conformation of (a) **3a** and (b) **3b** in their crystal structures.

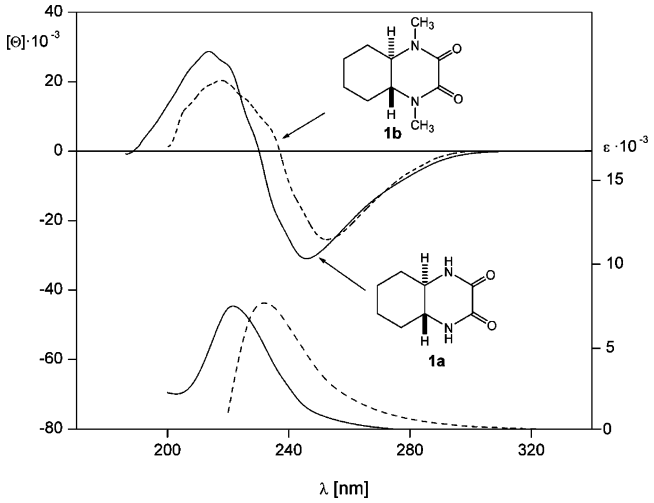

FIGURE 2. CD and UV (lower curves) spectra of **1a** and **1b** taken in methanol.

The calculated and experimental ring geometries of 2,3-piperazinedithiones **1c**−**6c** are generally similar to those of their parent dioxo derivatives (Table 1). The only difference is a much stronger twisting of the dithionooxamide unit as shown by the S═C−C═S torsion angles of ca. 40°, which reflect the relative steric size of oxygen and sulfur.

Chiroptical Spectra. The electronic absorption spectra of 2,3-piperazinediones **1a**,**b**−**3a**,**b** resemble those reported for other oxamides and are characterized by two absorption bands in the near-UV region: one intense band appearing as a maximum near 225 nm with a marked vibronic fine structure and the second of moderate intensity appearing as a shoulder near 250 nm (Figure 2). According to Larson and McGlynn,[7c] both these bands can be assigned to two allowed $\pi-\pi^*$ electronic transitions as supported by their large molecular extinction and the solvent red shift exhibited in highly polar media. In all cases, N-alkylation produces a considerable red shifting of the absorption bands. The spectra of **4a**,**b**−**6a**,**b** containing phenyl substituents are influenced by a contribution from the strong aromatic ring excitations. The oxamide chromophore can be viewed as being composed of two interacting amide units that results in splitting of the n, π, and π^* levels, and according to the ab initio calculations and photoelectron spectra, the ordering of the highest occupied molecular orbitals is π_-, n_+, π_+, and n_-, where the + and − subscripts indicate the bonding/antibonding combination of the parent amide orbitals.[7e] Besides two allowed $\pi-\pi^*$ transitions, the CNDO/s-CI calculations predict an additional forbidden $n-\pi^*$ excitation at slightly lower energies.[7b] It easily can be identified as a weak absorption at 272 nm in the UV spectrum of oxamide in aqueous solution. However, in the case of 2,3-piperazinodiones, this weak absorption band is buried under the tail of the much stronger $\pi-\pi^*$ transition and cannot be detected in the UV spectrum. Fortunately, the chiroptical spectra are very useful for the detection of hidden electronic transitions, and for example, the CD spectrum of **1b** taken in nonpolar solvents revealed the $n-\pi^*$ excitation as a very weak negative CE at 310 nm (see Figure 13S in the Supporting Information).

The CD spectra of cyclic oxamides **1a**,**b**−**6a**,**b** collected in Table 2 feature two strong CEs of opposite signs in accordance with the opposite symmetry of the excited states involved in two $\pi-\pi^*$ electronic transitions. In the case of skewed π electron systems, usually the inherent chirality of the chromophores controls the sign and magnitude of the CEs.[15] Examples are provided by cisoidal dienes,[16] helicenes,[17] skewed α-diketones,[18] or dithiooxalates.[19] Hug and Wagniere[20] postulated that the chromophores with C_2 symmetry and P-helicity produce negative CEs associated with the transitions of A symmetry and positive CEs for transitions of B symmetry, and the opposite signs are expected for the *M*-helicity. The rigid bicyclic skeleton of the C_2 symmetric molecules **1a** and **1b** implies the M-helicity of the twisted oxamide chromophore [O═C−C═O is −18.7(4)° in the crystals of **1a**], and thus, a sequence of the observed negative and positive CEs corresponding to the lower and higher energy $\pi-\pi^*$ transitions suggests their B and A symmetries, respectively. Similarly, the *P*-chirality of the chromophore in the bicyclic system **2b** results in reversed signs of two $\pi-\pi^*$ CEs. Thus, a simple helicity rule can be proposed for predictions of the CD sign of twisted oxamides: the right-handed chirality of the chromophore should lead to sequence positive and negative CEs corresponding to the lower and higher energy $\pi-\pi^*$ electronic transitions (Scheme 3). This explains correctly the observed CE signs for all of the compounds studied. Whereas the CD sign and magnitude of the conformationally rigid compounds **1a**,**b** largely are insensitive to substitution at the nitrogen atoms, the CD curves of oxamide **3a** and its *N*,*N*′-dimethyl derivative **3b** show opposite CE signs (Figure 3).

Since the inherent chirality of the skewed oxamide unit is primarily responsible for the CE sign and a contribution from the dissymmetrically located substituents is less important, the observed CD signs point to an opposite helicity of the chromophores in these compounds: the left-handed in **3a** and

(15) (a) Snatzke, G.; Snatzke, F. In *Fundamental Aspects and Recent Developments in Optical Rotatory Dispersion and Circular Dichroism*; Ciardelli, F., Salvadori, P., Eds.; Heyden: London, 1973, pp 109−125 and 173−195. (b) Snatzke, G. *Angew. Chem., Int. Ed. Engl.* **1979**, *18*, 363.
(16) Gawronski, J. K.; Walborsky, H. M. In *Circular Dichroism, Principles and Applications*; Nakanishi, K., Berova, N., Woody, R. W., Eds.; Wiley-VCH: New York, 1994; pp 301−304.
(17) Lightner, D. A.; Gurst, J. E. *Organic Conformational Analysis and Stereochemistry from Circular Dichroism Spectroscopy*; Wiley-VCH: New York, 2000; pp 409−421.
(18) Ibid, pp 305−335.
(19) Falth, L.; Hakansson, U.; Sandström, J. *J. Mol. Struct.* **1989**, *186*, 239.
(20) Hug, W.; Wagniere, G. *Tetrahedron* **1972**, *28*, 1241.

TABLE 2. Electronic Absorption (UV−vis) and CD Data

compd	solvent[a]	λ, nm (ϵ)	λ, nm (10^{-3} [Θ])[c]
1a	MeOH	248 (1190sh[b]), 221 (7710)	245 (−31.3), 214 (29.7)
1b	CD	246 ((3350sh[b]), 226 (8900)	310 (−0.031), 253 (−25.5), 218 (20.4)
	MeOH	253 (2520sh[b]), 232 (7830)	253 (−30.0), 215 (16.4)
1c	CD	480 (98), 422 (840), 315 (11800), 280 (3700sh[b])	509 (6.1), 424 (−16.5), 308 (−32.3), 270 (15.2), 250 (−3.7), 228 (31.9)
2a	MeOH	250 (2900sh[b]), 222 (11870)	249 (48.2), 217 (−25.3)
2b	CM	509 (80), 424 (406), 316 (7893), 280 (2530sh[b])	517 (−5.9), 424 (20.8), 308 (27.7), 259 (−22.0)
3a	H_2O	244 (1800sh[b]), 218 (10800)	242 (−10.9), 210 (7.1)
3b	H_2O	250 (2530sh[b]), 222 (10260)	249 (29.1), 220 (−16.6)
3c	CD	470 (80), 418 (725), 312 (12370), 275 (2770sh[b])	495 (−7.6), 418 (20.8), 307 (35.8), 263 (−19.1), 243 (9.2), 225 (−28.7)
4a	MeOH	244 (2200sh[b]), 211 (12050)	234 (−8.8), 225 (−9.3)
4b	MeOH	248 (3150sh[b]), 218 (11930)	253 (17.6), 222 (−31.9)
4c	CM	495 (128), 426 (732), 319 (11045)	513 (−8.1), 425 (28.6), 306 (32.0), 266 (−24.6), 246 (17.2), 227 (−32.3)
5a	MeOH	247 (4020sh[b]), 209 (22100)	248 (11.9), 218 (−33.3)
5b	MeOH	253 (3650sh[b]), 209 (23230)	254 (−49.2), 225 (34.9)
5c	CM	504 (73), 424 (690), 320 (1640)	510 (15.9), 426 (−38.7), 316 (−25.7), 270 (19.3), 245 (−68.1)
6a	MeOH	254 (1040sh[b]), 208 (8850)	253 (−1.6), 228 (+)[d]
6b	MeOH	253 (2470sh[b]), 213 (13330)	254 (−39.0), 224 (28.4)
6c	CD	504 (92), 422 (810), 316 (15080)	503 (24.9), 422 (−67.8), 307 (−102.7), 264 (77.2), 244 (−23.3), 228 (125)

[a] CD, cyclohexane/dioxane (4:1) and CM, cyclohexane/dichloromethane (4:1). [b] sh: Shoulder. [c] Molar ellipticity in deg cm^2 $dmol^{-1}$. [d] CD sign only was determined.

SCHEME 3

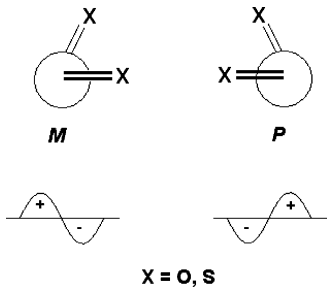

the right-handed in **3b**. This means that **3a** prefers the equatorial conformation in solution and **3b** the axial one, similar to the solid state. Furthermore, the magnitudes of the CEs in the spectrum of **3b** are roughly 3 times stronger than those in the spectrum of **3a** and comparable to those in the conformationally rigid compound **1b**, which suggests an overwhelming contribution of the axial form of **3b** to the conformational equilibrium. Analogous conformational preferences were observed for **4a**,**b** and **5a**,**b** (i.e., a predominance of the equatorial form in the case of the NH derivatives and the axial one for the *N*-methyl derivatives). As was already mentioned, a strong steric interaction between the *N*-methyl groups and the bulky equatorial substituents at C-5 and C-6 is primarily responsible for destabilization of the equatorial form. Particularly, a predominance of the diequatorial form of the diphenyl derivative **5a** observed in solution remains in variance with the solid state structure of the solvate **5a·THF**. However, the diaxial orientation of substituents is apparently due to the crystal packing of the solvate, and the crystals of the complex with pentafluorobenzoic acid (**pfb**) contain the diequatorial conformer of **5a**. Oxamide **6a** behaves exceptionally, where the CD spectrum suggests the axial orientation of the benzyl substituent in solution; however, the magnitudes of both CEs are rather small, which points to only a slight predominance of the axial form over the equatorial one in the conformational equilibrium.

The CD spectrum of **1c** (Figure 4) and the remaining dithiooxamides show at least six bands with alternating signs at the visible and near-UV region. Because of a similarity of the electronic structures of the oxamide and dithiooxamide chromophores, there is a close correspondence between their lowest energy transitions.

However, a substitution of sulfur for oxygen carbonyls results in bathochromic shifts and a better resolution of the absorption and CD bands in the spectra of dithiooxamides **1c**−**6c**. The UV−vis spectrum of **1c** reveals a weak absorption at 480 nm (ϵ 98) and a moderate intensity band at 422 nm (ϵ 840) in hydrocarbon solvents, and the absorptions shift to shorter wavelengths (470 and 395 nm, respectively) after the solvent is changed to methanol. Both these bands can be attributed to two forbidden $n-\pi^*$ electronic transitions. A strong absorption at 315 nm (ϵ 11 800), a position of which is almost independent of solvent polarity according to the energy-level diagram for the excited states proposed by Sandström and co-workers, can be attributed to two overlapping $\pi-\pi^*$ transitions,[7b] whereas a shoulder at 275 nm (ϵ 3700) is of less clear origin. A mutual correspondence between the CE signs of the third and fourth bands in the CD spectrum of **1c** and two $\pi-\pi^*$ bands in **1a**,**b** points to a similar origin of the corresponding excitations in both classes of compounds. Thus, exactly the same helicity rule as that for oxamides (Scheme 3) also can be used for the correlation of configuration of dithiooxamides. Indeed, the CE signs of the analogous CD bands in dithiooxamides **1c**−**6c** are the same as those of the $\pi-\pi^*$ CEs in their parent oxo compounds **1b**−**6b** (Table 2). This means that the conformational preferences of the dithionocarbonyl compounds **1c**−**6c** resemble those of their oxo analogues and, particularly, a predominance of the axial conformations in the case of **3c**−**6c** as confirmed by the crystal structures of **3c** and **6c**. In contrast to oxamides, where the weak $n-\pi^*$ CE can be observed with difficulty, their dithiono analogues show two relatively strong $n-\pi^*$ bands: one diffuse near 500 nm and the second of the opposite sign near 420 nm. The opposite sequence of the CEs to those of the $\pi-\pi^*$ bands suggests that the corresponding excited states have B and A symmetry, respectively. These CD bands have generally the same diagnostic value for stereochemical predictions as the CEs corresponding to the $\pi-\pi^*$ excitations.

Molecular Self-Assembly. Oxamides are superb hydrogen-bonding compounds[21] and have found a broad application in the design and synthesis of new molecular solids. The majority of the investigated structures contain a *trans*-oxamide function-

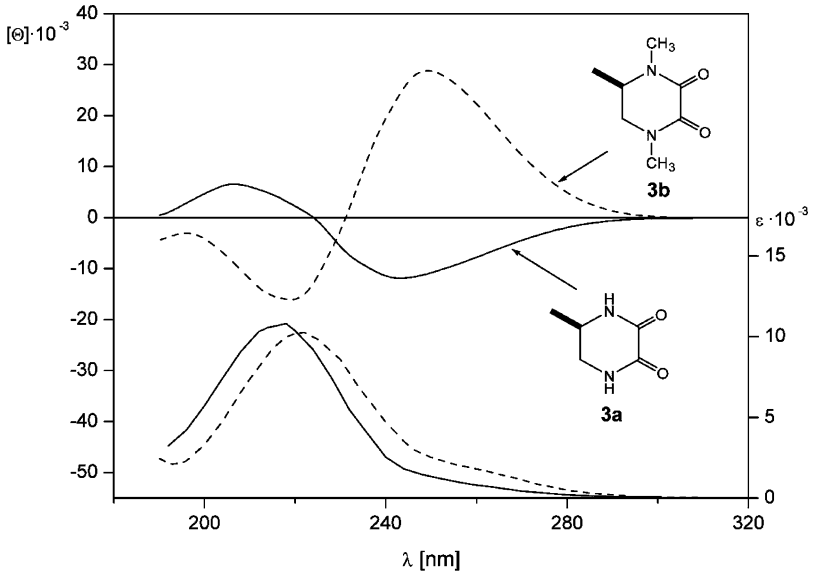

FIGURE 3. CD and UV (lower curves) spectra of **3a** and **3b** taken in water.

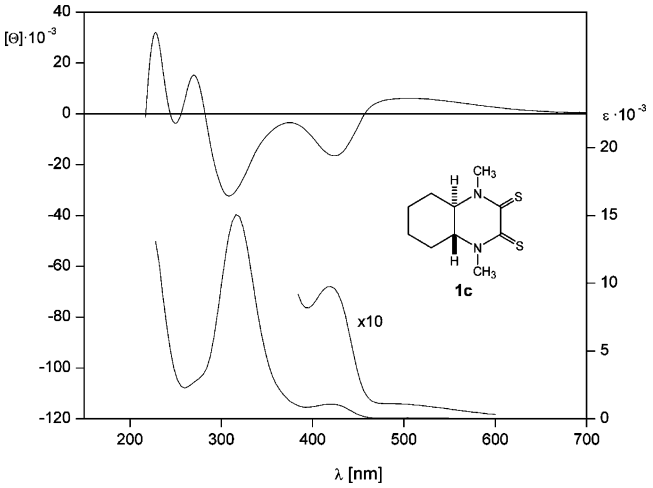

FIGURE 4. CD and UV−vis (lower curve) spectra of **1c** taken in cyclohexane−dioxane (4:1).

ality, and only a few structures containing *cis*-oxamide functions have been reported.[22] Cyclic oxamides are noncentrosymmetric units, and their hydrogen-bonded crystalline aggregates having a polar order are potentially useful because of their important physical properties.[23] Obtaining optically active 2,3-piperazinediones prompted us to take a closer look at their assembly mode in their homochiral crystals.

Compounds **1a** and **4a** crystallize in the space group $P4_32_12$, which may suggest the formation of hydrogen-bonded helical structures running along a 4-fold screw axis. Indeed, the common feature of these two structures is left-handed helices extended along the *c*-axis. In both crystals, the NH···O═C

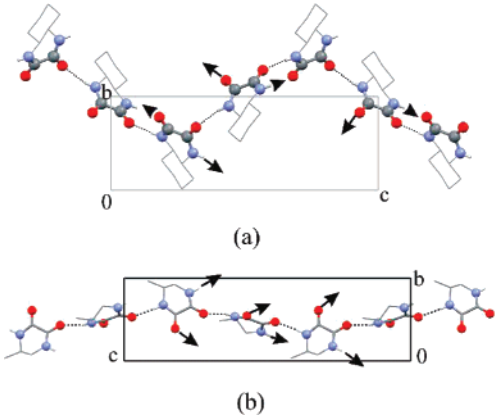

FIGURE 5. Left-handed helical structures extending along the 4_3 screw axis in the tetragonal crystals of (a) **1a** and (b) **3b**. Each oxalamide molecule takes part in two C(5) hydrogen-bond motifs: one extending along the helix axis and the second indicated by the arrows.

hydrogen bonds create a C(5) hydrogen-bond motif,[24] assembling molecules into a 3-D network (Figure 5). This motif is generated by the hydrogen bonds between two different amide units of the cyclic oxamide system: one acting as a donor and the second as an acceptor. In the crystals of **1a**, each constituent molecule of C_2 symmetry belongs to two 4_3 helices that leads to a 3-D hydrogen-bond network (see Figures 11aS and 12aS in the Supporting Information). In contrast, the molecules of **3a** are asymmetric, and two different types of the C(5) hydrogen-bond motifs are generated, one helical as shown in Figure 5 and the second extended perpendicularly to it, along the 2-fold screw axes, running parallel to the *ab*-diagonals (see Figures 11bS and 12bS in the Supporting Information). This helical assembly mode seems to be the preferred one for homochiral cyclic oxalamides with relatively small substituents located at C-5 and C-6. A completely different crystal packing was observed in the solvated crystal of **5a**, where the oxalamide

(21) (a) Coe, S.; Kane, J. J.; Nguyen, T. L.; Toledo, L. M.; Wininger, E.; Fowler, F. W.; Lauher, J. W. *J. Am. Chem. Soc.* **1997**, *119*, 86. (b) Nguyen, T. L.; Scott, A.; Dinkelmeyer, B.; Fowler, F. W.; Lauher, J. W. *New J. Chem.* **1998**, 129. (c) Nguyen, T. L.; Fowler, F. W.; Lauher, J. W. *J. Am. Chem. Soc.* **2001**, *123*, 11057.

(22) MacDonald, J. C.; Whitesides, G. M. *Chem. Rev.* **1994**, *94*, 2383.

(23) (a) Velsko, S. P. In *Materials for Nonlinear Optics. Chemical Perspectives*; Marder, S. R., Sohn, J. E., Stucky, G. D., Eds.; ACS Symposia Series 455; American Chemical Society: Washington, DC, 1991; pp 343−359. (b) Evans, O. R.; Lin, W. *Acc. Chem. Res.* **2002**, *35*, 511.

(24) For details of the definition, terminology, and notation in the graph set approach, see: (a) Etter, M. C. *Acc. Chem. Res.* **1990**, *23*, 120. (b) Bernstein, J.; Davis, R. E.; Shimoni, L.; Chang, N.-L. *Angew. Chem., Int. Ed. Engl.* **1995**, *34*, 1555.

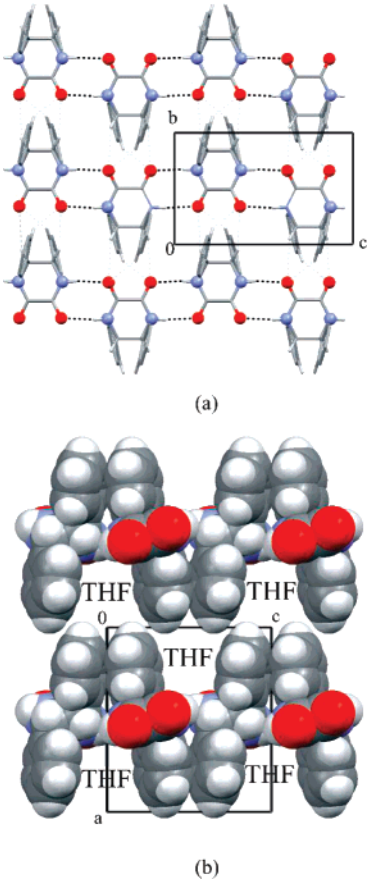

FIGURE 6. (a) Layer-type assemblies via N—H···O═C (black dashed lines) and C—H···O═C (gray dashed lines) interactions in **5a·THF** and (b) side view of the layers showing channels filled with the solvent molecules.

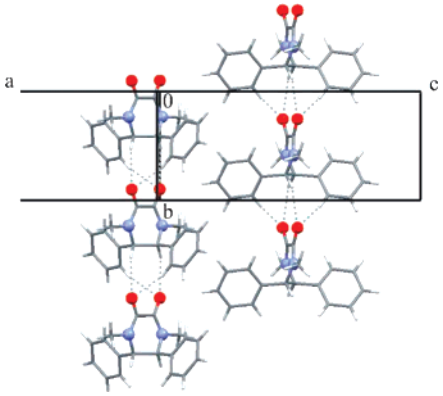

FIGURE 7. Molecular 1-D assemblies via C—H···O═C (gray dashed lines) interactions in **5b**. The crystal contains two such polymeric structures that are symmetry independent. Notice the similarity with **5a·THF**, where the analogue assemblies via C—H···O═C interactions are formed.

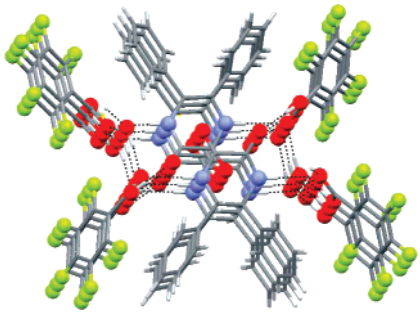

FIGURE 8. Hydrogen-bonded 1-D assembly of component molecules in **5a·fba$_2$·H$_2$O**; view along the *b*-axis.

molecule of the crystallographic C_2 symmetry assumed a diaxial conformation. In this case, the NH···O═C hydrogen bonds generate the cyclic motif $R_2^2(8)$, which assembles the molecules into tapes running parallel to the *c*-axis (Figure 6a). The tapes are further connected by a set of weaker C—H···O═C interactions into layers arranged parallel to (100). There are deep grooves formed between the phenyl rings protruding on both sides of the layer, which are, however, too narrow to accommodate the bumps from the adjacent layers. Since a closely packed structure cannot be formed, the layers of **5a** create a host matrix with channels extended along the *b*-axis that are filled with the THF molecules (Figure 6b). Interestingly, in the crystals of the *N*,*N*′-dimethyl derivative **5b**, where classical hydrogen bonds cannot be formed, weak C—H···O═C interactions assemble the molecules in a manner analogous to that observed in the crystal structure of **5a·THF** (Figure 7). It appeared that oxamide **5a** easily formed a hydrated complex **5a·pfb$_2$·H$_2$O** upon cocrystallization with pentafluorobenzoic acid from CH_2Cl_2. As mentioned earlier, in this case, the molecules of **5a** adopt a diequatorial conformation, in contrast to **5a·THF**, where the phenyl substituents are axially oriented. In this complex, the constituent molecules are connected via NH···O and OH···O hydrogen bonds into a 1-D polymeric structure extending along the *b*-axis (Figure 8). In this case, the oxalamide molecule acts simultaneously as a hydrogen-bond donor and acceptor to the **pfb** unit, whereas the water molecule binds only to the carboxyl group. Surprisingly, the $\pi-\pi$ stacking interactions between phenyl and electron deficient pentafluorophenyl rings,[25] which we considered to be a potential driving force for the complex formation, are absent since the centroid-to-centroid distances between phenyl and pentafluorophenyl rings are longer than 4.2 Å.

In conclusion, 2,3-piperazinodiones being simple models of *cis*-oxamides can be prepared easily by the condensation of 1,2-diamines with diethyl oxalate. The heterocyclic six-membered ring may assume two enantiomeric half-chair conformations with the twisted oxamide chromophore. Substitution at C-5 shifts the conformational equilibrium toward the equatorial conformer, whereas substitution at the nitrogen atoms results in domination of the axial form. Since the axial and equatorial conformers are characterized by the opposite helicity of the twisted oxamide chromophore, the changes in conformational equilibrium can be easily monitored by CD spectroscopy. Particularly, the CE signs corresponding to two allowed $\pi-\pi^*$ transitions were determined by the inherent chirality of the chromophore and can be predicted by the helicity rule. The same rule is also valid for 2,3-piperazinodithiones, where the substitution of sulfur for oxygen in the carbonyl groups results in bathochromic shifts and better resolution of the absorption and CD bands.

The crystal packing analysis of several homochiral 2,3-piperazinodiones revealed that strong NH···O═C intermolecular hydrogen-bonding interactions generating the C(5) chain motif resulted in the formation of supramolecular hydrogen-bonded helices as in the case of homochiral compounds with small

(25) (a) Gdaniec, M.; Jankowski, W.; Milewska, M. J.; Po-bński, T. *Angew. Chem., Int. Ed.* **2003**, *42*, 3903. (b) Piotrkowska, B.; Gdaniec, M.; Połoński, T. *CrystEngComm* **2007**, *9*, 868.

equatorially placed substituents or as in the case of the compounds with larger axially oriented substituent polymeric tapes with the use of the cyclic $R_2^2(8)$ hydrogen-bond motif.

Experimental Section

^{1}H and ^{13}C NMR spectra were obtained at 300 and 50 MHz, respectively, and the deuterated solvents were used as an internal lock.

(9*R*,10*R*)-2,3-Decahydrobenzopyrazinodione (1a). To a solution of (1*R*,2*R*)-(−)-1,2-diaminocyclohexane (1.8 g, 15 mmol) in EtOH (200 mL), diethyl oxalate (2.1 mL, 15 mmol) was added, and the mixture was refluxed for 3 h. The reaction mixture was filtered, the solvent was evaporated, and the product was crystallized from ethanol−water, 1.57 g (75%), mp >300 °C (lit.[26] racemate mp 301−303 °C); $[\alpha]_D^{22}$ −87.3 (*c* 2, 50% EtOH); ^{1}H NMR (DMSO-d_6) δ 8.58 (s, 2H), 3.19 (m, 2H), 1.84 (m, 2H), 1.64 (m, 2H), 1.22 (m, 4H); ^{13}C NMR (DMSO-d_6) δ 158.6, 54.9, 28.7, 23.0; ν_{max} (KBr)/cm^{-1} 3251, 1703, 1672. Anal. calcd for $C_8H_{12}N_2O_2$ (168): C, 57.13; H, 7.19; N, 16.66. Found: C, 57.10; H, 7.28; N, 16.83.

(9*R*,10*R*)-1,4-Dimethyl-2,3-decahydrobenzopyrazinodione (1b). A mixture of (1*R*,2*R*)-(−)-*N*,*N*′-dimethyl-1,2-diaminocyclohexane[27] (1.47 g, 15 mmol) and diethyl oxalate (1.5 mL, 10 mmol) in toluene (50 mL) was refluxed for 5 h. After the addition of heptane crystallized the product, 1.6 g (82%), mp 154 °C; $[\alpha]_D^{22}$ −150.7 (*c* 2, $CHCl_3$); ^{1}H NMR ($CDCl_3$) δ 3.38 (m, 2H), 3.06 (s, 6H), 2.32 (m, 2H), 1.92 (m, 2H), 1.45−1.30 (complex m, 4H); ^{13}C NMR ($CDCl_3$) δ 157.9, 58.4, 28.6, 28.4, 23.4; ν_{max} (KBr)/cm^{-1} 1703, 1672. Anal. calcd for $C_{10}H_{16}N_2O_2\cdot H_2O$ (205): C, 58.53; H, 8.29; N, 13.65. Found: C, 58.58; H, 8.35; N, 13.56.

(9*R*,10*R*)-1,4-Dimethyl-2,3-decahydrobenzopyrazinodithione (1c). Oxamide **1b** (1.0 g, 5 mmol) and Lawesson's reagent (2.4 g, 6 mmol) were refluxed in toluene (20 mL) for 90 min. After evaporation of the solvent, the residue was subjected to column chromatography on silica gel, and elution with $CDCl_3$ gave 0.95 g (83%) of the product; mp 236−238 °C; $[\alpha]_D^{20}$ +812.5 (*c* 0.2, $CHCl_3$). ^{1}H NMR ($CDCl_3$) δ 3.57 (s, 6H), 3.43 (m, 2H), 2.48 (m, 2H), 1.95 (m, 2H), 1.55 (m, 2H), 1.37 (m, 2H); ^{13}C NMR ($CDCl_3$) δ 188.5, 61.1, 37.8, 28.9, 23.6; ν_{max} (KBr)/cm^{-1} 1469, 1358, 1235. Anal. calcd for $C_{10}H_{16}N_2S_2$ (228): C, 52.59; H, 7.06; N, 12.27; S, 28.08. Found: C, 52.66; H, 7.18; N, 12.18; S, 28.09.

(*S*)-2-Methylhexahydropyrrolo[1,2-*a*]pyrazine-3,4-dione (2b). Bicyclic oxamide **2b** was prepared from (*S*)-2-[*N*-methyl(aminomethyl)]pyrrolidine[28] in the same manner as compound **1b**; yield 75%; mp 178−180 °C, $[\alpha]_D^{25}$ +154.5 (*c* 0.662, $CHCl_3$); ^{1}H NMR ($CDCl_3$) δ 4.02 (m, 1H), 3.66−3.58 (m, 2H), 3.46 (d, *J* = 5.2 Hz, 1H), 3.06 (s, 3H), 2.26−2.02 (m, 2H), 2.0−1.8 (m, 2H), 1.68−1.56, m, 1H); ^{13}C NMR ($CDCl_3$) δ 158.7, 155.7, 55.1, 52.8, 45.5, 35.4, 30.5, 23.6; ν_{max} (KBr)/cm^{-1} 1674. Anal. calcd for $C_8H_{12}N_2O_2$ (168): C, 57.13; H, 7.19; N, 16.66. Found: C, 57.04; H, 7.13; N, 16.48.

(*S*)-2-Methylhexahydropyrrolo[1,2-*a*]pyrazine-3,4-dithione (2c). The previous oxamide (1.0 g, 5.95 mmol) and Lawesson's reagent (2.64 g, 6.54 mmol) were refluxed in toluene (70 mL) for 2 h. The reaction mixture was allowed to cool to room temperature, and the brown precipitate was removed by filtration to give the title compound. Yield 0.91 g (76.5%); mp 209−211 °C (ethanol), $[\alpha]_D^{25}$ −480 (*c* 0.136, $CHCl_3$); ^{1}H NMR ($CDCl_3$) δ 4.0 (br s, 1H), 3.89 (m, 2H), 3.8−3.64 (m, 2H), 3.58 (s, 3H), 2.33 (br s, 1H), 2.21 (br s, 1H), 2.04 (br s, 1H), 1.78 (br s, 1H); ^{13}C NMR ($CDCl_3$) δ 186.7, 182.9, 57.5, 55.6, 54.1, 45.4, 30.8, 23.2; ν_{max} (KBr)/cm^{-1} 1487, 1374. Anal. calcd for $C_8H_{12}N_2S_2$: C, 47.97; H, 6.04; N, 13.98; S, 32.01. Found: C, 47.96; H, 6.00; N, 13.97; S, 32.09.

(*R*)-5-Methyl-2,3-piperazinodione (3a). Compound **3a** was prepared from (*R*)-1,2-diaminopropane[29] in a similar manner to that of **1a** in 92% yield; mp 205−209 °C; $[\alpha]_D^{25}$ −78.8 (*c* 1, MeOH);^{1}H NMR (DMSO-d_6) δ 8.55 (s, 1H), 8.48 (s, 1H), 3.70 (m, 1H), 3.28 (m, 1H), 3.08 (m, 1H), 1.11 (d, *J* = 6.9 Hz, 3H); ^{13}C NMR (DMSO-d_6) δ 162.1, 49.6, 49.3, 22.0; ν_{max} (KBr)/cm^{-1} 3210, 1657. Anal. calcd for $C_5H_8N_2O_2$ (128): C, 46.87; H, 6.29; N, 21.86. Found: C, 46.93; H, 6.27; N, 22.06.

(*R*)-1,4,5-Trimethyl-2,3-piperazinodione (3b). Compound **3b** was prepared from (*R*)-*N*,*N*′-dimethyl-1,2-diaminopropane[27,30] in a similar manner to that of **1b** in 79% yield; mp 115−116 °C; $[\alpha]_D^{20}$ +100 (*c* 0.4, $CHCl_3$); ^{1}H NMR ($CDCl_3$) δ 3.92 (dd, *J* = 12.8 and 4.4 Hz, 1H), 3.59 (m, 1H), 3.13 (dd, *J* = 12.8 and 2.9 Hz, 1H), 3.11 (s, 3H), 3.07 (s, 3H), 1.38 (d, *J* = 6.8 Hz, 3H); ^{13}C NMR ($CDCl_3$) δ 155.9, 155.7, 50.5, 50.3, 33.9, 31.7, 15.6; ν_{max} (KBr)/cm^{-1} 1685, 1492. Anal. calcd for $C_7H_{12}N_2O_2$ (156): C, 53.83; H, 7.74; N, 17.94. Found: C, 53.63; H, 7.78; N, 18.04.

(*R*)-1,4,5-Trimethyl-2,3-piperazinodithione (3c). Thionation of **3b** with Lawesson's reagent in toluene afforded the product in 85% yield; mp 148 °C; $[\alpha]_D^{20}$ −886 (*c* 0.2, $CHCl_3$); ^{1}H NMR ($CDCl_3$) δ 4.04 (dd, *J* = 13.8 and 3.9 Hz, 1H), 3.82 (m, 1H), 3.61 (s, 3H), 3.55 (s, 3H), 3.41 (dd, *J* = 13.8 and 1.9 Hz, 1H), 1.38 (d, *J* = 6.8 Hz, 3H); ^{13}C NMR ($CDCl_3$) δ 184.8, 184.7, 54.0, 53.7, 44.3, 42.0, 14.4, ν_{max} (KBr)/cm^{-1} 1495, 1313. Anal. calcd for $C_7H_{12}N_2S_2$ (188): C, 44.65; H, 6.43; N, 14.88; S, 34.05. Found: C, 44.68; H, 6.62; N, 15.04; S, 34.25.

(*R*)-5-Phenyl-2,3-piperazinedione (4a). Compound 4**a** was prepared from (*R*)-1,2-diamino-1-phenylethane[31] in a similar manner to that of **1a** in 92% yield; mp >220 °C (dec); $[\alpha]_D^{22}$ −87.7 (*c* 0.114, DMSO); ^{1}H NMR (DMSO-d_6) δ 8.97 (s, 1H, NH), 8.45 (s, 1H, NH), 7.40 (t, *J* = 7.5 Hz, 2H), 7.33 (m, 3H), 4.78 (s, 1H), 3.66 (m, 1H), 3.39 (m, 1H); ν_{max} (KBr)/cm^{-1} 3296, 1656. Anal. calcd for $C_{10}H_{10}N_2O_2$ (190): C, 63.15; H, 5.30; N, 14.73. Found: C, 63.39; H, 5.52; N, 14.93.

(*R*)-1,4-Dimethyl-5-phenyl-2,3-piperazinedione (4b). To a stirred suspension of **4a** (2.5 g, 13.15 mmol) in anhydrous THF (120 mL), sodium hydride (1.5 g, 37.5 mmol, 60% dispersion in mineral oil) was added. After being stirred for 15 min, methyl iodide (2.46 mL, 39.5 mmol) was added in one portion, and the reaction mixture was stirred overnight. The excess of NaH was quenched by the slow addition of water, and the product was extracted with ethyl acetate. The organic layer was dried ($MgSO_4$), and the solvent was removed under reduced pressure. The residue was crystallized from ethyl acetate-diethyl ether: yield 1.5 g, (52%); mp 197−200 °C, $[\alpha]_D^{22}$ −42.9 (*c* 0.14, $CHCl_3$); ^{1}H NMR ($CDCl_3$) δ 7.39 (m, 3H), 7.23 (d, *J* = 6.8 Hz, 2H), 4.61 (t, *J* = 3.9 Hz, 1H), 4.07 (dd, *J* = 12.9 and 4.6 Hz, 1H), 3.41 (dd, *J* = 13.2 and 3.4 Hz, 1H), 3.0 (s, 3H), 2.92 (s, 3H); ^{13}C NMR ($CDCl_3$) δ 158.2, 157.6, 136.9, 129.5, 129.1, 126.6, 60.3, 53.2, 35.4, 34.2; ν_{max} (KBr)/cm^{-1} 1681. Anal. calcd for $C_{12}H_{14}N_2O_2$ (218): C, 66.04; H, 6.47; N, 12.84. Found: C, 65.93; H, 6.42; N, 12.76.

(*R*)-1,4-Dimethyl-5-phenyl-2,3-piperazinedithione (4c). Thionation of **4b** with Lawesson's reagent in toluene afforded brown needles of the product in 68% yield; mp 152−154 °C (ethanol); $[\alpha]_D^{22}$ −677 (*c* 0.096, $CHCl_3$); ^{1}H NMR ($CDCl_3$) δ 7.38 (d, *J* = 6.8 Hz, 3H), 7.19 (d, *J* = 6.3 Hz, 2H), 4.85 (br s, 1H), 4.36 (dd, *J* = 13.7 and 3.4 Hz, 1H), 3.73 (d, *J* = 12.2 Hz, 1H), 3.53 (s, 3H), 3.34 (s, 3H); ^{13}C NMR ($CDCl_3$) δ 187.7, 186.4, 135.0, 129.7, 129.4,

(26) Brill, E.; Schultz, H. P. *J. Org. Chem.* **1963**, *28*, 1135.
(27) Kashiwabara, K.; Hanaki, K.; Fujita, J. *Bull. Chem. Soc. Jpn.* **1980**, *53*, 2275.
(28) (a) Betschart, C.; Schmidt, B.; Seebach, D. *Helv. Chim. Acta* **1988**, *71*, 1999. (b) Bose, D. S.; Lakshminarayana, V. *Tetrahedron Lett.* **1998**, *39*, 5631. (c) Trotter, N.; Brimble, M. A.; Harris, P. W. R.; Callis, D. J.; Sieg, F. *Bioorg. Med. Chem.* **2005**, *13*, 501.
(29) Dwyer, F. P.; Garvan, F. L.; Shulman, A. *J. Am. Chem. Soc.* **1959**, *81*, 290.
(30) Trethof, J. A.; Cooke, D. W. *Inorg. Nucl. Chem. Lett.* **1972**, *8*, 1013.
(31) (a) Belokon, Y. N.; Pritula, L. K.; Tararov, V. I.; Bakhmutov, V. I.; Struchkov, Y. T. *J. Chem. Soc., Dalton Trans.* **1990**, *6*, 1867. (b) Lagriffoul, P.-H.; Tadros, Z.; Taillades, J.; Commeyras, A. *J. Chem. Soc., Perkin Trans 2* **1992**, 1279. (c) Wang, M.-X.; Lin, S.-J. *J. Org. Chem.* **2002**, *67*, 6542.

126.5, 62.9, 56.2, 45.6, 44.2; ν_{max} (KBr)/cm^{-1} 1491, 1344, 1297. Anal. calcd for $C_{12}H_{14}N_2S_2$ (250): C, 57.56; H, 5.64; N, 11.19; S, 25.61. Found: C, 57.66; H, 5.72; N, 11.09; S, 25.56.

(5*S*,6*S*)-5,6-Diphenyl-2,3-piperazinedione (5a). The title compound was prepared from (1*S*,2*S*)-(−)-1,2-diamino-1,2-diphenylethane following the procedure analogous to that of **1a**; yield 82%; mp 222−224 °C, $[\alpha]_D^{22}$ −58.3 (*c* 0.24, DMSO); ^{1}H NMR (DMSO-d_6) δ 8.85 (br s, 2H, NH), 7.32 (m, 10H), 4.80 (t, J = 2.4 Hz, 2H); ^{13}C NMR (DMSO-d_6) δ 158.4, 139.6, 128.5, 127.9, 126.8, 59.6; ν_{max} (KBr)/cm^{-1} 3368, 1708. Anal. calcd for $C_{16}H_{14}N_2O_2$ (266): C, 72.17; H, 5.30; N, 10.52. Found: C, 72.11; H, 5.35; N, 10.44.

(5*S*,6*S*)-1,4-Dimethyl-5,6-diphenyl-2,3-piperazinedione (5b). N-Methylation of **5a** following the procedure analogous to that of **4b** afforded the title product in 68% yield; mp 262−264 °C (methanol−diethyl ether), $[\alpha]_D^{22}$ −84.8 (*c* 0.33, $CHCl_3$); ^{1}H NMR ($CDCl_3$) δ 7.42 (m, 6H), 7.28 (m, 4H), 4.55 (s, 2H), 2.86 (s, 6H); ^{13}C NMR ($CDCl_3$) δ 157.4, 137.4, 129.4, 128.9, 125.9, 67.4, 34.5; ν_{max} (KBr)/cm^{-1} 1668. Anal. calcd for $C_{18}H_{18}N_2O_2$ (294): C, 73.45; H, 6.16; N, 9.52. Found: C, 73.24; H, 6.15; N, 9.46.

(5*S*,6*S*)-1,4-Dimethyl-5,6-diphenyl-2,3-piperazinedithione (5c). Thionation of **5b** with Lawesson's reagent in toluene afforded the title product in 65% yield; mp 231−233 °C (toluene−hexane); $[\alpha]_D^{22}$ +685 (*c* 0.054, $CHCl_3$); ^{1}H NMR ($CDCl_3$) δ 7.40 (m, 6H), 7.30 (m, 4H), 4.87 (s, 2H), 3.34 (s, 6H); ^{13}C NMR ($CDCl_3$) δ 186.7, 135.6, 129.6, 129.2, 126.0, 69.9, 44.8; ν_{max} (KBr)/cm^{-1} 1492, 1394, 1287. Anal. calcd for $C_{18}H_{18}N_2S_2$ (326): C, 66.22; H, 5.56; N, 8.58; S, 19.64. Found: C, 66.28; H, 5.39; N, 8.57; S, 19.60.

(*S*)-5-Benzyl-2,3-piperazinedione (6a). The oxamide **6a** was prepared from (*S*)-1,2-diamino-3-phenylpropane[32] in a manner similar to that of **1a** and had a mp >250 °C (dec), $[\alpha]_D^{22}$ −82.2 (*c* 0.073, DMSO); ^{1}H NMR (DMSO-d_6) δ 8.71 (br s, 1H, NH), 8.45 (br s, 1H, NH), 7.18−7.38 (m,5H), 3.76 (br s, 1H), 3.16 (m, 1H), 3.08 (m, 1H), 2.93 (m, 1H), 2.73 (m, 1H); ^{13}C NMR (DMSO-d_6) δ 158.9, 158.7, 137.7, 129.9, 129.2, 127.3, 51.7, 43.0, 39.0; ν_{max} (KBr)/cm^{-1} 3287, 1654. Anal. calcd for $C_{11}H_{12}N_2O_2$ (204): C, 64.69; H, 5.92; N, 13.72. Found: C, 64.33; H, 6.04; N, 13.44.

(*S*)-1,4-Dimethyl-5-benzyl-2,3-piperazinedione (6b). N-Methylation of **6a** following the procedure analogous to that of **4b** afforded the title product in 70% yield; mp 126−129 °C; $[\alpha]_D^{22}$ −78.6 (*c* 0.458, $CHCl_3$); ^{1}H NMR ($CDCl_3$) δ 7.36 (t, J = 7.3 Hz, 2H), 7.29 (t, J = 7.3 Hz, 1H), 7.15 (d, J = 7.3 Hz, 2H), 3.81 (dd, J = 13.2 and 4.4 Hz, 1H), 3.55 (m, 1H), 3.12 (dd, J = 13.7 and 5.4 Hz, 1H), 3.08 (d, J = 1.5 Hz, 1H), 3.06 (s, 6H), 2.88 (dd, J = 13.7 and 10.5 Hz, 1H); ^{13}C NMR ($CDCl_3$) δ 157.6, 157.2, 136.6, 129.4, 129.3, 127.6, 58.6, 48.2, 37.5, 35.3, 34.4; ν_{max} (KBr)/cm^{-1} 1685. Anal. calcd for $C_{13}H_{16}N_2O_2$ (232): C, 67.22; H, 6.94; N, 12.06. Found: C, 67.25; H, 6.93; N, 11.95.

(*S*)-1,4-Dimethyl-5-benzyl-2,3-piperazinedithione (6c). Thionation of **6b** with Lawesson's reagent in toluene afforded the title product in 66% yield; mp 148−151 °C (toluene−hexane);

$[\alpha]_D^{22}$ +800 (*c* 0.08, $CHCl_3$); ^{1}H NMR ($CDCl_3$) δ 7.37 (t, J = 7.3 Hz, 2H), 7.29 (t, J = 7.3 Hz, 1H), 7.16 (d, J = 7.6 Hz, 2H), 3.79 (dd, J = 14.2 and 3.9 Hz, 1H), 3.83 (m, 1H), 3.57 (s, 3H), 3.38 (s, 3H), 3.38 (dd, J = 14.2 and 1.5 Hz, 1H), 3.09 (dd, J = 13.7 and 6.8 Hz, 1H), 2.82 (dd, J = 13.7 and 9.03 Hz, 1H); ^{13}C NMR ($CDCl_3$) δ 186.5, 186.3, 135.8, 129.5, 129.3, 127.9, 61.7, 51.9, 45.5, 44.5, 36.4; ν_{max} (KBr)/cm^{-1} 1493, 1392, 1330. Anal. calcd for $C_{13}H_{16}N_2S_2$ (264): C, 59.05; H, 6.10; N, 10.59; S, 24.25. Found: C, 59.21; H, 6.11; N, 10.67; S, 24.11.

X-ray data were collected with a KM4CCD diffractometer. The crystal structures were solved by direct methods with SHELXS97[33] and refined by full-matrix least-squares SHELXL97.[34] All structural drawings were prepared with the program Mercury, version 1.4.2.[35]

Crystal Data for $C_8H_{12}N_2O_2$ (1a). M = 168.20, tetragonal, space group $P4_32_12$, a = b = 6.6090(3) Å, c = 18.8339(15) Å, V = 822.64(8) Å^3, T = 293 K, Z = 4, ρ_x = 1.358 g cm^{-3}, μ(Mo−Kα) = 0.099 mm^{-1}, λ = 0.71073 Å, 3290 reflections measured, 584 unique (R_{int} = 0.0206). Final residuals for 56 parameters were R_1 = 0.0367, wR_2 = 0.0865 for 483 reflections with $I > 2\sigma(I)$, and R_1 = 0.0471, wR_2 = 0.0962 for all data.

Crystal Data for $C_5H_8N_2O_2$ (3a). M = 128.13, tetragonal, space group $P4_32_12$, a = b = 6.9810(1) Å, c = 24.2018(7) Å, V = 1179.46(4) Å^3, T = 293 K, Z = 8, ρ_x = 1.443 g cm^{-3}, μ(Mo−Kα) = 0.113 mm^{-1}, λ = 0.71073 Å, 7224 reflections measured, 781 unique (R_{int} = 0.0141). Final residuals for 82 parameters were R_1 = 0.0282, wR_2 = 0.0702 for 719 reflections with $I > 2\sigma(I)$, and R_1 = 0.0316, wR_2 = 0.0736 for all data.

Crystal Data for $C_7H_{12}N_2O_2$ (3b). M = 156.19, orthorhombic, space group $P2_12_12_1$, a = 7.8934(2) Å, b = 9.0440(2) Å, c = 11.2187(3) Å, V = 800.88(3) Å^3, T = 120 K, Z = 4, ρ_x = 1.295 g cm^{-3}, μ(Mo−Kα) = 0.096 mm^{-1}, λ = 0.71073 Å, 10 437 reflections measured, 959 unique (R_{int} = 0.0229). Final residuals for 103 parameters were R_1 = 0.0304, wR_2 = 0.0793 for 881 reflections with $I > 2\sigma(I)$, and R_1 = 0.0338, wR_2 = 0.0828 for all data.

Crystal Data for $C_7H_{12}N_2S_2$ (3c). M = 188.31, orthorhombic, space group $P2_12_12_1$, a = 6.4030(12) Å, b = 11.526(2) Å, c = 12.735(3) Å, V = 939.9(3) Å^3, T = 140 K, Z = 4, ρ_x = 1.331 g cm^{-3}, μ(Mo−Kα) = 0.507 mm^{-1}, λ = 0.71073 Å, 7126 reflections measured, 1902 unique (R_{int} = 0.0820). Final residuals for 102 parameters were R_1 = 0.0402, wR_2 = 0.0936 for 1833 reflections with $I > 2\sigma(I)$, and R_1 = 0.0422, wR_2 = 0.0949 for all data.

Crystal Data for $C_{16}H_{14}N_2O_2 \cdot C_4H_8O$(5a·THF). M = 338.40, orthorhombic, space group $P222_1$, a = 12.405(2) Å, b = 6.9058-(10) Å, c = 11.0030(12) Å, V = 942.6(2) Å^3, T = 200 K, Z = 2, ρ_x = 1.192 g cm^{-3}, μ(Mo− Kα) = 0.081 mm^{-1}, λ = 0.71073 Å, 4202 reflections measured, 988 unique (R_{int} = 0.0390). Final residuals for 116 parameters were R_1 = 0.0590, wR_2 = 0.1558 for 635 reflections with $I > 2\sigma(I)$, and R_1 = 0.0942, wR_2 = 0.1846 for all data. The solvent molecule is strongly disordered. At 195 K, the crystal exhibited a phase transition to a triclinic twinned phase.

Crystal Data for $C_{16}H_{14}N_2O_2 \cdot 2(C_7HF_5O_2) \cdot H_2O$(5a·fba$_2$·H$_2$O). M = 708.46, monoclinic, space group $P2_1$, a = 14.4997(15) Å, b = 5.9482(7) Å, c = 16.7914(17) Å, β = 94.631(9)°, V = 1443.5-(3) Å^3, T = 100 K, Z = 2, ρ_x = 1.630 g cm^{-3}, μ(Mo− Kα) = 0.158 mm^{-1}, λ = 0.71073 Å, 12062 reflections measured, 3228 unique (R_{int} = 0.0356). Final residuals for 460 parameters were R_1 = 0.0297, wR_2 = 0.0526 for 2256 reflections with $I > 2\sigma(I)$, and R_1 = 0. 0.0600, wR_2 = 0.0633 for all data.

Crystal Data for $C_{18}H_{18}N_2O_2$ (5b). M = 294.34, monoclinic, space group $C2$, a = 23.6192(10) Å, b = 6.7822(3) Å, c = 16.8873-(6) Å, β = 119.234(4)°, V = 2360.63(19) Å^3, T = 200 K, Z = 6, ρ_x = 1.242 g cm^{-3}, μ(Mo−Kα) = 0.082 mm^{-1}, λ = 0.71073 Å, 6125 reflections measured, 2600 unique (R_{int} = 0.0390). Final residuals for 302 parameters were R_1 = 0.0314, wR_2 = 0.0794 for 2134 reflections with $I > 2\sigma(I)$, and R_1 = 0. 0.0415, wR_2 = 0.0867 for all data.

Crystal Data for $C_{13}H_{16}N_2O_2$ (6b). M = 232.28, orthorhombic, space group $P2_12_12_1$, a = 7.3532(5) Å, b = 8.6308(6) Å, c = 18.8901(13) Å, V = 1198.84(14) Å^3, T = 140 K, Z = 4, ρ_x = 1.287 g cm^{-3}, μ(Mo−Kα) = 0.088 mm^{-1}, λ = 0.71073 Å, 9998 reflections measured, 1594 unique (R_{int} = 0.0378). Final residuals

(32) (a) Brunner, H.; Schmidt, M.; Unger, G.; Schoenenberger, H. *Eur. J. Med. Chem.* **1985**, *20*, 509. (b) Taillades, J.; Boussac, P.; Collet, H.; Brugidou, J.; Commeyras, A. *Bull. Soc. Chim. Fr.* **1991**, *3*, 423. (c) Tandon, V. K.; Yadav, D. B.; Singh, R. V.; Chaturvedi, A. K.; Shukla, P. K. *Bioorg. Med. Chem. Lett.* **2005**, *15*, 5324.

(33) Sheldrick, G. M. *Acta Crystallogr., Sect. A: Found. Crystallogr.* **1990**, *46*, 467.

(34) Sheldrick, G. M. *SHELXL-97: Program for the Refinement of a Crystal Structure from Diffraction Data*; University of Göttingen: Göttingen, Germany, 1997.

(35) Macrae, C. F.; Edgington, P. R.; McCabe, P.; Pidcock, E.; Shields, G. P.; Taylor, R.; Towler, M.; van de Streek, J. *J. Appl. Crystallogr.* **2006**, *39*, 453−457.

for 156 parameters were $R_1 = 0.0365$, $wR_2 = 0.0811$ for 1368 reflections with $I > 2\sigma(I)$, and $R_1 = 0.0485$, $wR_2 = 0.0862$ for all data.

Crystal Data for $C_{13}H_{16}N_2S_2$ [6c(I)]. $M = 264.40$, orthorhombic, space group $P2_12_12$, $a = 10.2156(11)$ Å, $b = 14.1494(12)$ Å, $c = 9.4788(8)$ Å, $V = 1370.1(2)$ Å^3, $T = 130$ K, $Z = 4$, $\rho_x = 1.282$ g cm^{-3}, μ(Mo−Kα) = 0.369 mm^{-1}, $\lambda = 0.71073$ Å, 13 976 reflections measured, 2421 unique ($R_{int} = 0.0344$). Final residuals for 156 parameters were $R_1 = 0.0288$, $wR_2 = 0.0591$ for 2226 reflections with $I > 2\sigma(I)$, and $R_1 = 0.0376$, $wR_2 = 0.0616$ for all data. These crystals (red prisms) and crystals of **6c**(II) (orange needles) appeared as concomitant polymorphs. Recrystallization from toluene−hexane mixture afforded only crystals of the form **6c**(I).

Crystal Data for $C_{13}H_{16}N_2S_2$ [6c(II)]. $M = 264.40$, monoclinic, space group $P2_1$, $a = 7.2071(18)$ Å, $b = 15.029(3)$ Å, $c = 13.526(4)$ Å, $\beta = 104.71(2)°$, $V = 1417.0(6)$ Å^3, $T = 130$ K, $Z = 4$, $\rho_x = 1.239$ g cm^{-3}, μ(Mo− Kα) = 0.356 mm^{-1}, $\lambda = 0.71073$ Å, 9236 reflections measured, 4272 unique ($R_{int} = 0.0360$). Final residuals for 311 parameters were $R_1 = 0.0438$, $wR_2 = 0.0784$ for 3396 reflections with $I > 2\sigma(I)$, and $R_1 = 0.0625$, $wR_2 = 0.0849$ for all data.

Acknowledgment. We are indebted to Dr. J. Frelek (IChO PAN, Warsaw) for CD measurements with use of her JASCO J-715 instrument. Financial support from the Committee of Scientific Research (Project 3 T09A 030 29) is gratefully acknowledged.

Supporting Information Available: ^{1}H and ^{13}C NMR spectra for all new compounds, ORTEP plots, crystal packing diagrams for **1a**, **3a**, **6c**(I), and **6c**(II), and atomic coordinates for computed structures. This material is available free of charge via the Internet at http://pubs.acs.org.

JO800037W